Journal of Sedimentary Research

Journal of Sedimentary Research, 2006, v. 76, 310–323
Research Article
DOI: 10.2110/jsr.2006.021

MORPHOLOGY OF MOLAR-TOOTH STRUCTURES IN PRECAMBRIAN CARBONATES: INFLUENCE OF SUBSTRATE RHEOLOGY AND IMPLICATIONS FOR GENESIS

MARK D. POLLOCK,[1] LINDA C. KAH,[1] AND JULIE K. BARTLEY[2]

[1]*Department of Earth & Planetary Sciences, University of Tennessee, Knoxville, Tennessee 37996, U.S.A.*
[2]*Department of Geosciences, State University of West Georgia, Carrollton, Georgia 30118, U.S.A.*
e-mail: lckah@utk.edu

ABSTRACT: **Molar-tooth (MT) is an enigmatic carbonate fabric composed of variously shaped cracks and voids filled with a characteristically uniform, equant microspar. MT is both abundant and widespread in Mesoproterozoic and early Neoproterozoic strata, where void-filling microspar comprises up to 90% of individual beds and 5–25% of preserved carbonate. The temporal restriction of this fabric suggests a potential link between MT formation and the biogeochemical evolution of marine environments. Detailed petrographic relationships among MT crack morphology, distribution of MT microspar, and composition of the surrounding substrate suggest that crack formation and microspar precipitation are intimately linked to the decomposition of sedimentary organic matter in the presence of supersaturated Proterozoic seawater.**

Laboratory experiments have shown that gas generated within unconsolidated mud can reproduce a variety of MT crack morphologies, yet current gas expansion and migration models do not explicitly consider the role of substrate variability in determining morphologies of MT cracks. A detailed petrographic examination of MT structures from the Mesoproterozoic Belt Supergroup, Montana, permits interpretation of the microscale relationship between crack morphology and lithologic, and potentially rheologic, variability of the surrounding substrate by tracing the distribution of petrographically distinctive MT microspar. Observations of lateral offset of MT cracks at bedding planes or within coarser-grained siltstone or sandstone layers, termination of cracks beneath clay- or organic-rich horizons, grain collapse into underlying MT cracks, and the presence of MT microspar as a pore-filling precipitate suggest that grain size, substrate lithology, and substrate cohesion all play critical roles in the development of MT cracks. By contrast, the presence of a wide range of MT crack morphologies within petrographically homogeneous substrates, and an apparent relationship between crack diameter and sinuosity, suggest that the void-forming process itself also played a role in determining the final morphology of MT cracks. Together, these petrographic observations are used to define a model of microscale gas–sediment interactions that can be used to interpret crack morphology in terms of gas pressure and the strength of sedimentary substrates.

The presence of characteristic, void-filling microspar is integral to preservation of MT structures. Cathodoluminescence (CL) identification of this characteristic microspar within MT voids, in pore space of coarse-grained facies, and interstitially within fine-grained facies adjacent to MT voids suggests that MT voids and cement share a common genesis. Because microspar cores are similar in size and morphology to vaterite precipitated experimentally in the presence of a variety of dissolved organic molecules, we suggest that precipitation of MT microspar was intimately linked with gas production during organic decomposition within the host substrate. In this scenario, gas production would result in pore fluids with elevated concentrations of dissolved organic molecules, which would initiate precipitation of MT microspar when the pore fluids come in contact with supersaturated Proterozoic seawater. Restriction of MT largely to Mesoproterozoic and early Neoproterozoic strata likely reflects a critical level of carbonate saturation that limited early substrate lithification, thereby allowing void production but remained high enough that organic catalysts were able to initiate precipitation of MT microspar.

INTRODUCTION

Molar-tooth (MT) structures are an unusual Precambrian carbonate fabric composed of variously oriented voids and cracks, filled with uniform microspar, that formed at or near the sediment–water interface (Smith 1968; O'Connor 1972). MT structures are both abundant and widespread in Mesoproterozoic to early Neoproterozoic subtidal to intertidal deposits (James et al. 1998), yet they occur only rarely in older or younger successions (e.g., Bishop and Sumner 2002). The temporal restriction of MT structures may provide clues to environmental conditions present during the Mesoproterozoic to early Neoproterozoic. However, at present, the applicability of MT structures as a tool for environmental interpretation is limited because their genesis is poorly understood.

The term "molar-tooth" was first used by Bauerman (1885) to describe vertical to horizontal, crenulate sheets of calcite in rocks of the Belt Supergroup, Montana, U.S.A., which he likened to enamel crenulations on the grinding surfaces of the molar teeth of elephants. In outcrop, MT

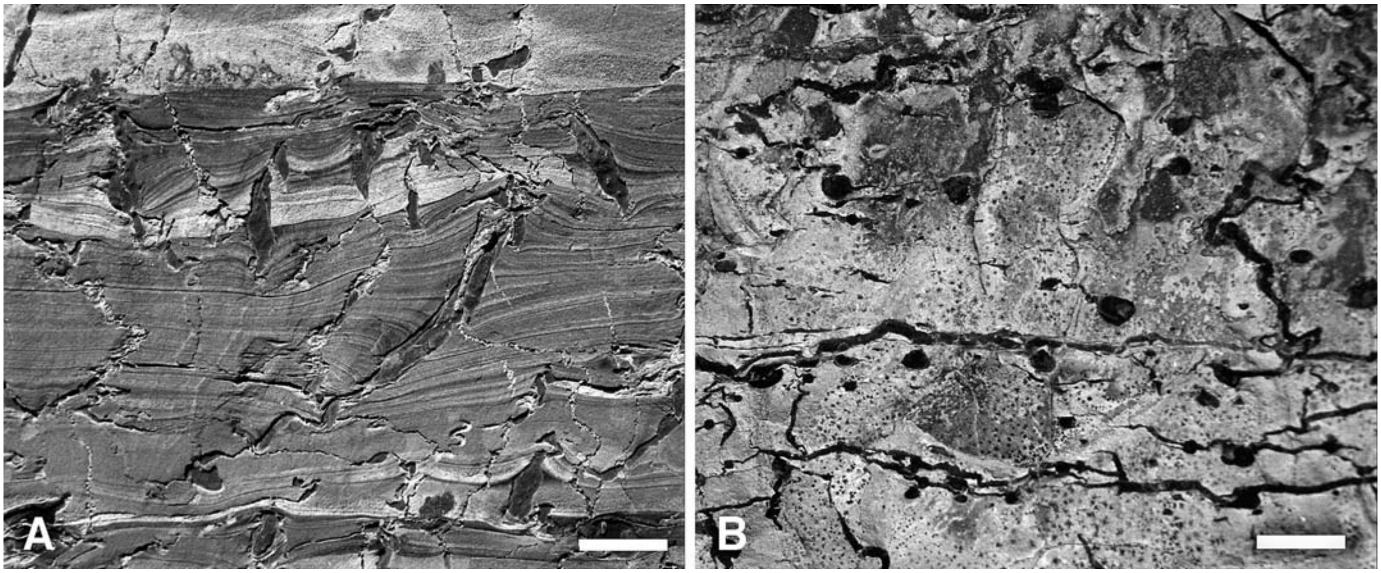

FIG. 1.—Morphologies of MT structures in the Mesoproterozoic Belt Supergroup. **A)** Compacted laminae around thick, straight, vertical ribbons demonstrates early lithification of MT voids. **B)** Spheroidal MT structures showing protrusions of ribbon morphologies that can link to ribbons forming complex networks. Scale bar is 1 cm in all photos.

structures are visible on weathered surfaces, where they appear as sharply bounded, light to dark gray, recessive features surrounded by buff-colored dolomitic lime mudstone. They occur predominantly within fine-grained, clay-bearing carbonate rocks and are generally absent or rare in siltstone and sandstone. The morphology of MT structures typically ranges from linear, sheet-like ribbons to spheroids ("blobs" of O'Connor 1972). MT ribbons occur as vertical to horizontal structures that are straight to crenulated, or ptygmatically folded to broken (Fig. 1A), and typically measure a few millimeters in width and a few centimeters to tens of centimeters in length. MT spheroids are ovoid to circular in cross section (Fig. 1B), are spheroidal in three dimensions, and measure a few millimeters to 1 cm in diameter. MT ribbons and spheroids occur together in outcrop, in cases pass from one morphology to the other, and frequently intersect in three dimensions to form interconnected networks (cf. Furniss et al. 1998; Pratt 1998). MT structures are filled with a distinctive carbonate microspar composed of uniform, equant crystals 5 to 15 μm in diameter that typically continues, without break, through interconnected voids (Frank and Lyons 1998; Furniss et al. 1998).

Combined, the morphology of MT structure and its relationship with surrounding sediment suggests that cracks formed in unlithified sediment, near the sediment–water interface, and that MT-filling microspar was precipitated soon after, and perhaps penecontemporaneously with, crack genesis. The unlithified nature of the substrate is demonstrated by compaction of substrate laminae around microspar-filled cracks (Fig. 1A; see also Smith 1968; Fairchild et al. 1997; Pratt 1998, 2001), which can show variable amounts of folding (Smith 1968; Calver and Baillie 1990) or *en echelon* breakage during compaction (Fairchild et al. 1997; Pratt 1998, 2001), suggesting rapid lithification of crack fill. MT cracks also typically lack detrital infill (Furniss et al. 1998), suggesting formation of cracks and precipitation of MT microspar mainly beneath the sediment–water interface. Lithified cracks, however, are commonly ripped up and redeposited as storm breccias (Furniss et al. 1998; Pratt 1998, 2001) and can be observed as ridges projecting upwards as erosional remnants into overlying sediment (O'Connor 1972; Furniss et al. 1998; Pratt 1998), indicating formation close to the top of the sediment column.

Any satisfactory hypothesis for the origin of MT structures must take into account three fundamental observations regarding the nature of MT voids and their fill: (1) MT voids occur as a variety of coexisting morphologies; (2) MT structures formed during earliest postdepositional diagenesis in unlithified sediment near the sediment–water interface; and (3) MT structures were lithified rapidly by carbonate microspar. With exception of a few works that examine the composition of MT microspar and its temporal distribution (Frank and Lyons 1998; James et al. 1998; Shields 2002), studies of MT have focused largely on potential void-forming mechanisms. These include tectonic fracturing (Daly 1912); replacement of algal (O'Connor 1972; Moussine-Pouchkine and Bertrand-Sarfati 1997) and evaporitic (Eby 1977) structures; mudcrack deformation (Demicco and Hardie 1994); synaeresis (Horodyski 1976; Young and Long 1977; Calver and Baillie 1990), diastasis (Cowan and James 1992; Smith and Winston 1997), sediment compaction (Bell 1966), or earthquake-induced dewatering (Fairchild et al. 1997; Pratt 1998, 2001), and gas expansion and migration (Furniss et al. 1998; Marshall and Anglin 2004).

A gas expansion and migration origin for MT voids, in which gas production and expansion within the host substrate is attributed to either the microbial decomposition of sedimentary organic matter (Furniss et al. 1998) or the destabilization of CO_2 clathrates in the shallow subsurface (Marshall and Anglin 2004), appears, at present, most compelling because it accounts satisfactorily for both a common origin for a wide variety of MT morphologies and for its early postdepositional formation in unlithified sediment near the sediment–water interface. A series of laboratory experiments, in which yeast and sugar were added to a water-saturated matrix of kaolinite mud, with or without plaster of Paris as a stiffening agent, demonstrated the viability of a gas expansion and migration hypothesis (Furniss et al. 1998). In these experiments, variation in MT void morphology was attributed primarily to differences in gas volume, although sediment stiffness and surface confinement may have also played a role in determining crack formation.

Unfortunately, current gas expansion and migration hypotheses (Furniss et al. 1998; Marshall and Anglin 2004) do not explicitly consider the role of substrate variability in determining MT void morphologies. In the field, MT structures possess a distinct set of crack morphologies that correspond broadly with depositional cycles, are repeated in successive depositional cycles, and can be traced laterally for long distances within the same facies (O'Connor 1972; Winston 1986; Fairchild et al. 1997; Winston and Lyons 1997; James et al. 1998). More detailed examination

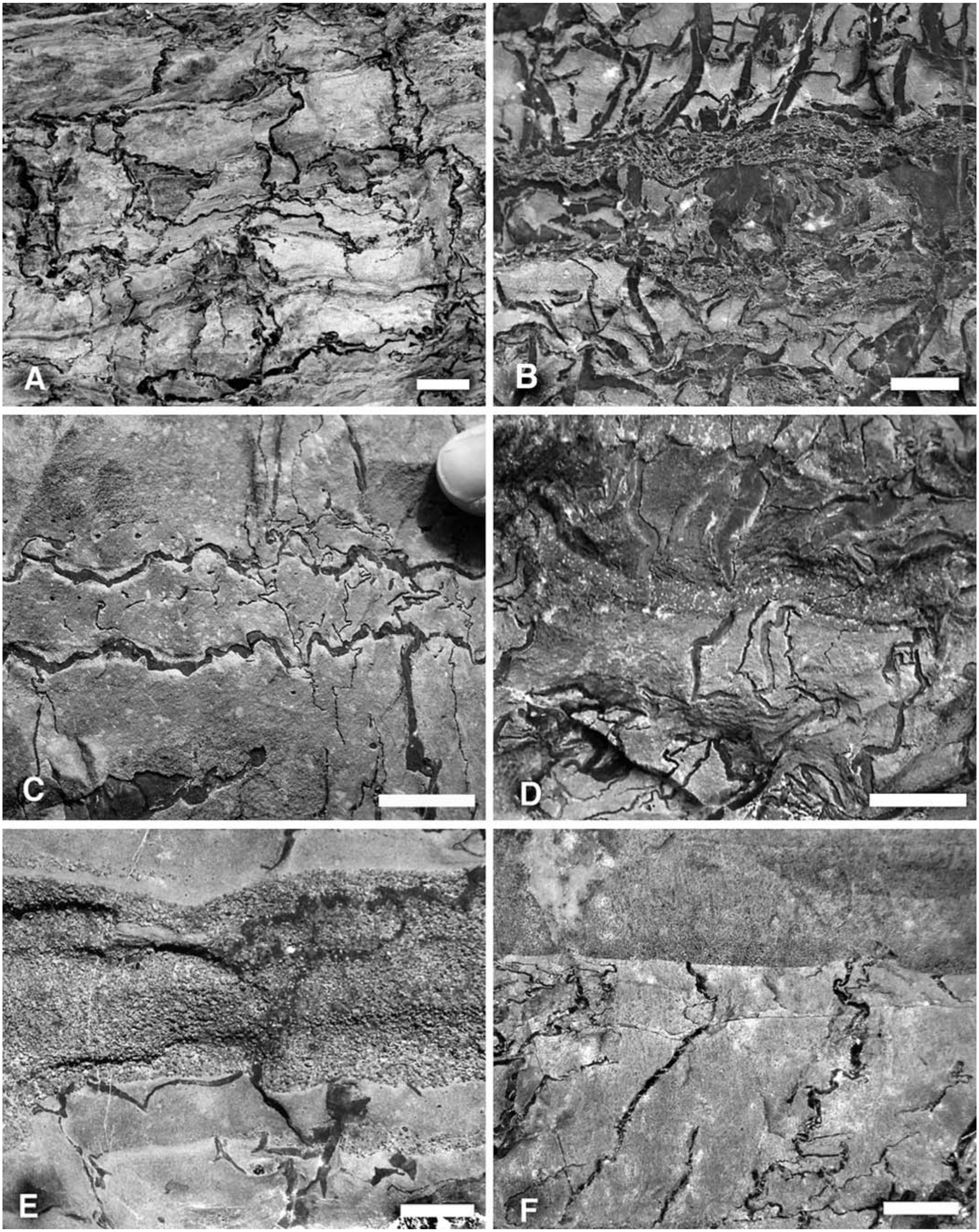
A
B
C
D
E
F

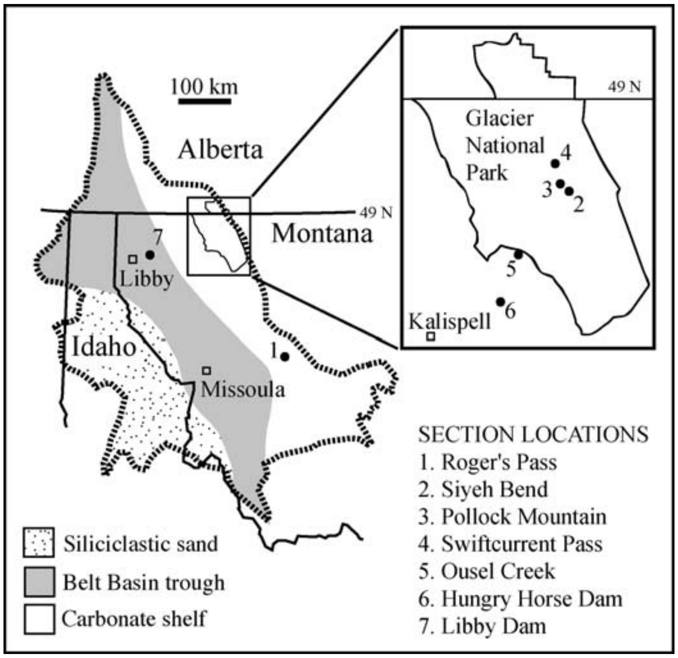

FIG. 3.— Location map for measured sections in the Helena Formation, Belt Supergroup, northern Montana.

of this pattern, from this study and others, suggests a strong relationship between the morphology of MT voids and substrate characteristics. Whereas MT ribbons occur in a variety of facies, MT spheroids are most common in clay-rich, fine-grained carbonate rocks (Fig. 1B; see also O'Connor 1972), and MT voids are typically absent from coarse siltstone, sandstone, and other coarse-grained facies (e.g., oolitic limestone; see also Smith 1968; Fairchild et al. 1997; Pratt 1998, 2001). Additionally, MT ribbons exhibit a variety of morphological changes both within single substrate lithologies and when ribbons intersect different lithologies. Typically, thinner ribbons (1–2 mm wide) are more sinuous (Fig 2A), whereas thicker ribbons show less morphological variability, except where they intersect and merge within microbial laminae (Fig 2B; see also O'Connor 1972; Pratt 1998). Thin ribbons frequently become horizontal, or offset, at lamina boundaries or within individual laminae (Fig 2C; see also Bell 1966; Smith 1968; O'Connor 1972; Fairchild et al. 1997), frequently pinch as they pass through thin sand layers (Fig 2D), and become diffuse within or terminate at thicker coarse-grained layers (Fig. 2E, F; see also Fairchild et al. 1997; Pratt 1998, 2001). These observations support a strong rheologic control on MT morphology.

In this paper, we provide a petrographic examination of MT structures from the Mesoproterozoic Helena Formation, Belt Supergroup, Montana, and explore the microscale relationship between crack morphology and lithologic, and potentially rheologic, variability of the surrounding substrate by tracing the distribution of petrographically distinctive MT microspar. We then examine the consistency of gas expansion and migration hypotheses of MT genesis (Furniss et al. 1998; Marshall and Anglin 2004) by constructing a conceptual model that considers grain-scale gas–sediment interactions and the observed relationships among MT crack morphology, distributions of MT microspar, and composition of the surrounding substrate.

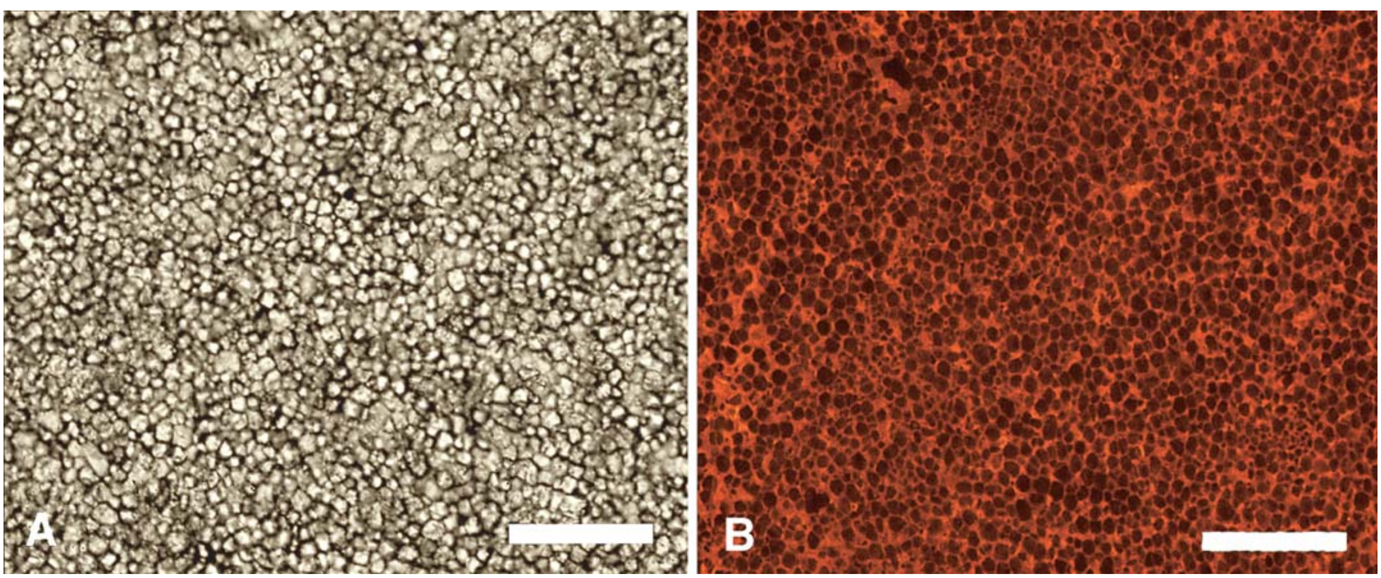

FIG. 4.—MT microspar. **A)** MT microspar composed of uniform, equant crystals ranging 5 to 15 µm in diameter and averaging 7 to 11 µm. **B)** Cathodoluminescence photomicrograph of MT microspar reveals crystals composed of dully luminescent, subrounded cores and more brightly luminescent, polygonal overgrowths. Scale bar is 100 µm in all photos.

←

FIG. 2.— Outcrop-scale changes in MT morphology. **A)** Thin vertical ribbons commonly display a highly sinuous morphology. **B)** Thick vertical ribbons become horizontal at substrate boundaries, here forming small, densely packed horizontal pockets within microbialite layers. **C)** Both thin and thick ribbons become predominantly horizontal within coarser-grained substrate layers. **D)** Vertical ribbons pinch and disappear as they pass through medium-grained sandstone layers. **E)** Well-defined vertical ribbons become irregular or diffuse within a coarse-grained oolite, until they reenter overlying fine-grained strata. **F)** Vertical ribbons thin, bend horizontally beneath, and disappear into a fine sandstone layer. Scale bar in all photos in 1 cm.

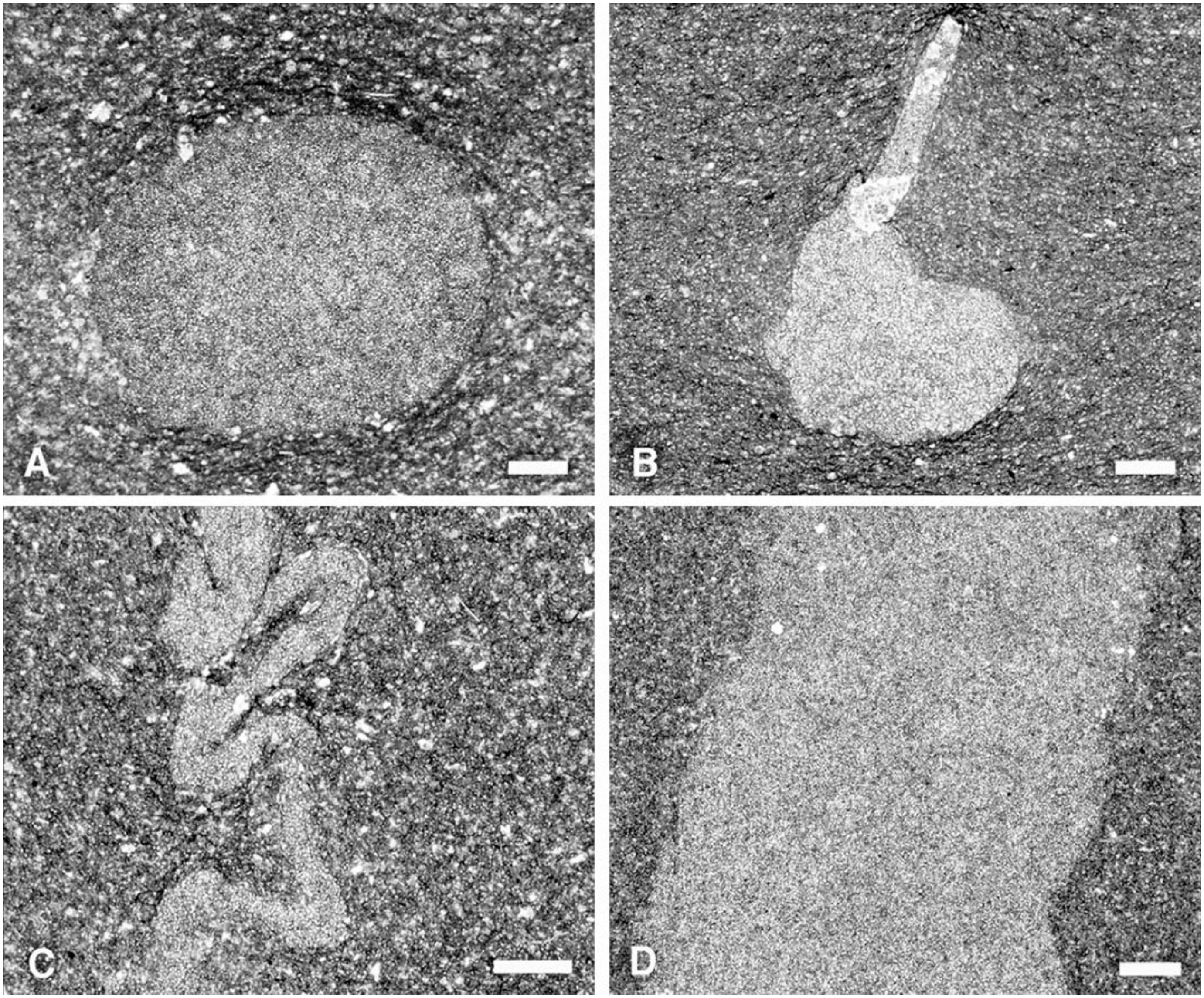

FIG. 5.—Continuum of MT morphologies in fine-grained strata. **A)** Spheroidal morphologies are interpreted to result from initial gas production when gas pressures initially overcome the strength of the surrounding substrate. **B)** Ribbon protrusions are interpreted to form where inhomogeneities in the sedimentary substrate affect the strength of grain–grain contacts and mark initial deformation of the substrate in response to increasing gas pressures. **C)** Thin, sinuous ribbons are interpreted to reflect pathways of migrating gas that are greatly affected by small changes in the intergranular strength of the substrate. **D)** Thick straight ribbons are interpreted to reflect gas pressures significantly greater than the strength of the surrounding substrate. Scale bar is 200 μm in all photos. All photos are in plane-polarized light.

GEOLOGIC FRAMEWORK

MT structures were observed and described from the 1.45 Ga Helena Formation (Evans et al. 2000), Belt Supergroup, Montana, U.S.A. (Fig. 3), which contains abundant MT and a range of MT morphologies (Bell 1966; Smith 1968; O'Connor 1972; Eby 1977; Furniss et al. 1998; Pratt 1998). The Helena Formation is ~ 800 m thick and is composed of upward-fining siliciclastic-to-carbonate cycles (1 to 10 m thick) that consist of a lower, argillaceous interval overlain by calcitic to dolomitic mudstone with interbedded grainstone, sandstone, and stromatolitic facies (Winston 1986; Winston and Lyons 1997). Cycles are frequently bounded by scoured surfaces and are interpreted to represent deposition in a shallow subtidal to intertidal setting (Horodyski 1983; Winston et al. 1984; Grotzinger 1986; Winston 1986). MT structures are most abundant within fine-grained, dolomitic cycle tops and are rare to absent in argillaceous cycle bases and coarse-grained intervals. The abundance of MT decreases westward in the basin, where the Helena Formation grades into the more argillaceous and deeper-water depositional environments of the Wallace Formation (Winston and Link 1993).

PETROGRAPHY

Molar-Tooth Microspar

In this study, the presence of MT microspar is used to define microscale relationships between MT structures and matrix sediment. Pratt (1998) interpreted MT microspar as geopetal "crystal silt" (Dunham 1969) that was segregated from the sediment matrix and transported to MT cracks during seismic shaking and liquefaction of the substrate. However, petrographic analysis indicates that MT microspar is distinguishable from the fine-grained carbonate that typically occurs within the sedimentary

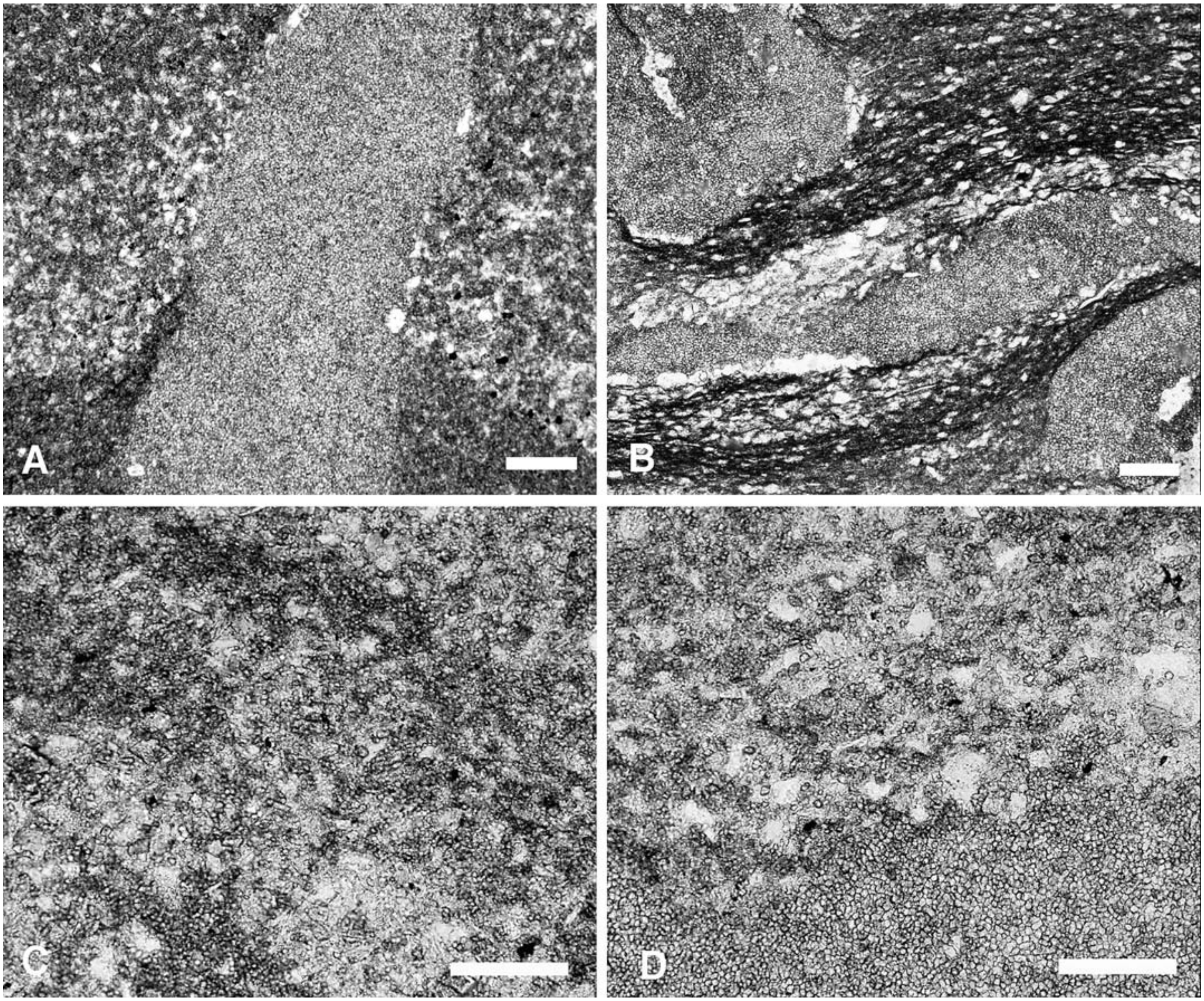

FIG. 6.—MT morphologies interpreted to result from changes in stratal composition. **A)** Vertical ribbon passing from fine-grained to coarse-grained layers with little change in morphology. **B)** Largely vertical ribbon (lower left) is displaced laterally within a coarse-grained layer prior to resuming its vertical path (upper right). **C)** Pore-filling MT microspar in a fine-grained sandstone. **D)** Pore-filling MT microspar in a fine-grained sandstone, above a well-defined horizontal MT ribbon. Scale bar is 200 μm in all photos. All photos are in plane-polarized light.

matrix. MT microspar is composed of uniform, equant, limpid crystals, 5 to 15 μm in diameter, that show planar crystalline boundaries (Fig. 4A) and sharp contacts with the surrounding host sediment (Figs. 5–8). By contrast, fine-grained carbonate within the sedimentary matrix (Figs. 5–8) typically shows a much larger range of crystal sizes (3 to > 50 μm in diameter), is cloudy in appearance, and contains a predominance of nonplanar crystal boundaries and a variable presence of sharply planar euhedral rhombs. When observed under cathodoluminescence (CL), distinction between MT microspar and fine-grained carbonate within the matrix becomes even more apparent. Under CL, MT microspar crystals show uniform, rounded 3–5 μm nonluminescent to dully luminescent cores surrounded by more brightly luminescent, polygonal rims (Fig. 4B). These luminescence characteristics suggest that MT microspar crystals originated as micrite-size, spheroidal particles that remained in suspension within the MT cracks (perhaps as a colloid) and provided nucleation points for later polygonal overgrowths, which filled remaining void space. Compaction of matrix sediment around fully lithified MT structures and the presence of storm-deposited intraclasts of MT microspar requires that precipitation of both initial spheroidal particles and later polygonal overgrowths occur during earliest postdepositional diagenesis. This two-stage history for MT microspar contrasts sharply with that of the majority of carbonate crystals within the sedimentary substrate, which preserves a much greater variability in grain size, grain shape, and CL characteristics. Although characteristic MT microspar occasionally occurs within the sedimentary matrix (Fig. 8A, B), most carbonate within the matrix consists of either cloudy, nonplanar (i.e., neomorphic) fabrics showing variably dull to bright luminescence, or euhedral dolomite rhombs showing multiply zoned luminescence, suggesting a more complex, multistage precipitation history.

Therefore, although MT microspar does not display fabrics typical of a precipitated carbonate cement (e.g., crystal orientation perpendicular to substrate walls, competitive growth boundaries, or inward-increasing

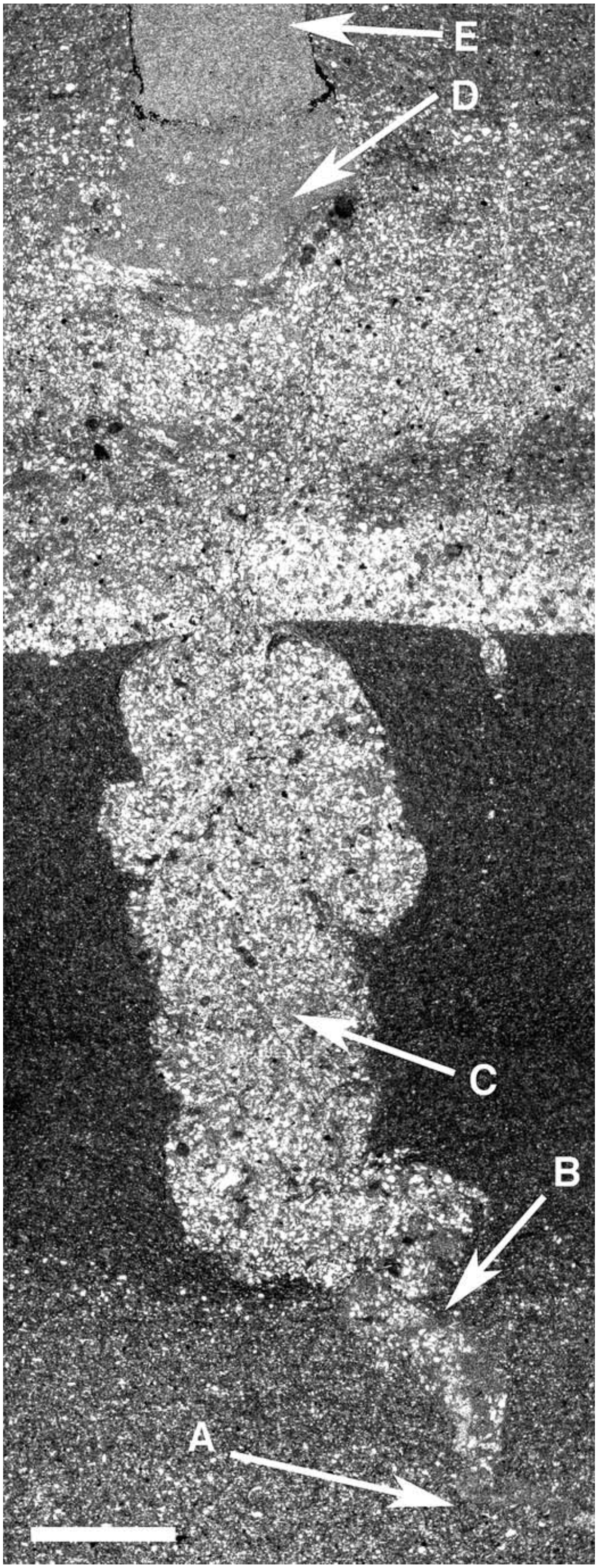

grain size), the combination of luminescence characteristics, uniform crystal sizes (Kile et al. 2000), and planar crystal contacts, and distinct crack boundaries suggest rapid heterogeneous nucleation and precipitation of microspar *in situ* within MT voids (Crawford and Kah 2004), perhaps as a colloidal suspension. A morphologically similar microspar has been noted to fill cavities within organic-walled fossils that are normally preserved as carbonaceous compressions (Hofmann 1985), and occasionally MT cracks contain well-preserved acritarchs, cyanobacterial filaments, and coccoidal microfossils (Furniss et al. 1998). In these cases, decomposition of the organic material would be expected to have proceeded within days to weeks of deposition (Bartley 1996), suggesting that precipitation of MT microspar must have occurred penecontemporaneously with or immediately after void formation.

Morphology of Molar-Tooth Cracks

The distinctive petrographic character of MT microspar facilitates recognition of MT cracks in thin section and helps to define the detailed relationships between MT cracks and the surrounding sedimentary substrate. Most MT occurs in a matrix consisting of dolomitic microspar containing 5–20% fine-grained quartz, and minor feldspar and clay. A full array of spheroidal and ribbon morphologies occur within such homogeneous substrates. Spheroidal structures (Fig. 5A) are typically a few millimeters in diameter and are occasionally bounded by a thin (25 to 50 μm) interval containing a concentration of clays aligned tangentially to the surface of the structure. MT ribbons commonly occur as small protrusions from MT spheroids (Fig. 5B). In homogeneous substrates, protrusions are typically oriented perpendicular to bedding; in strongly stratified rocks, protrusions are more frequently oriented parallel to bedding where they track bedding planes. Within homogeneous substrates, MT ribbons have both ptygmatically folded and straight morphologies (Fig. 5C, D) that are oriented roughly perpendicular to bedding. Where strongly folded and straight morphologies are adjacent to one another, the former are typically thinner (50 μm to several millimeters in diameter) than the latter (1 mm to nearly 1 cm in diameter) for any given substrate composition, although finer-grained and more clay-rich substrates appear to contain a greater proportion of straight ribbons.

In samples where obvious petrographic changes in substrate occur, MT ribbons typically show changes in morphology that coincide with changes in the sedimentary substrate. In rare cases, vertical ribbons pass from fine- to coarse-grained layers and show no change in width or direction. In these cases, lamina changes are subtle, often consisting of a greater proportion of silt- or sand-size material disseminated through the fine-grained carbonate (Fig. 6A). Where abrupt increases in grain size occur, vertical MT structures occasionally become horizontal and remain confined within coarse-grained layers for some distance before resuming a vertical path (Fig. 6B). Lateral deflection of MT structures is also common when MT ribbons intersect clay drapes or organic-rich laminae, where the fine-grained material appears to have acted as barriers to crack formation. In stratiform microbialites and stromatolites, lateral deflection of MT structures results in horizontal layers of closely packed, elongate

←

FIG. 7.—Intersection of a vertical MT ribbon with lithologies of differing grain size. The presence of MT microspar is disrupted by detrital filling by unconsolidated sand. Lowermost part of the crack is completely filled with MT microspar **(A)**; proportion of MT microspar decreases upward as detrital sand component increases **(B)**, until MT microspar is observed only as an precipitated phase interstitially to detrital sand **(C)**. Near the top of the sandstone layer, proportion of MT microspar increases dramatically **(D)** and the upper extension of the MT crack is, once again, completely filled with MT microspar **(E)**. Scale bar is 1 mm. Photo is in plane-polarized light.

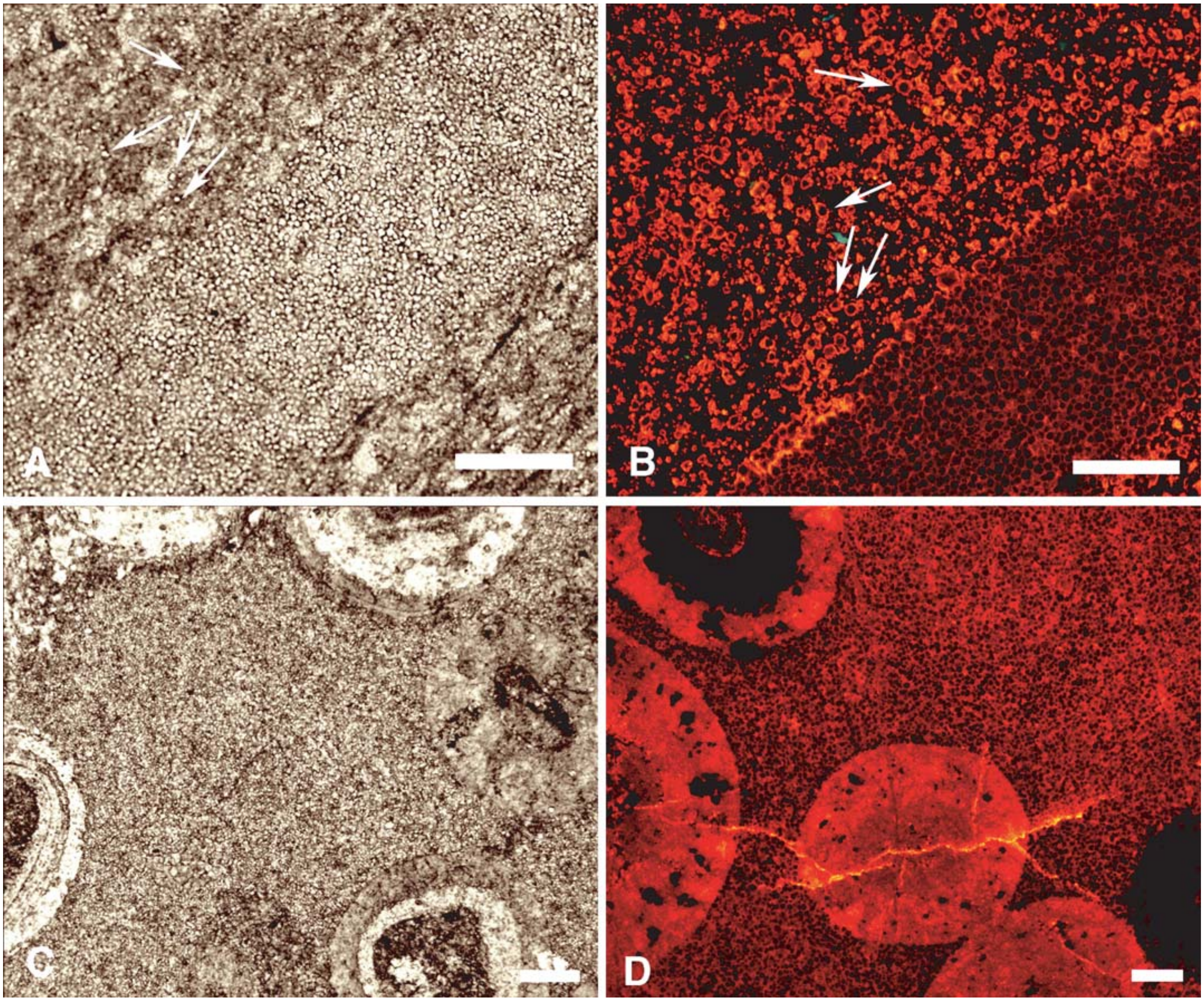

FIG. 8.— Evidence for gas interstitially within fine-grained sediment and at the sediment–water interface. **A)** Individual microspar crystals in fine-grained matrix surrounding a well-defined MT ribbon. **B)** Cathodoluminescence photomicrograph showing the characteristic two-phase construction of MT microspar. **C)** Microspar as the primary intergranular component of an oolitic grainstone. **D)** Cathodoluminescence photomicrograph showing the characteristic two-phase construction of MT microspar. Scale bar is 200 μm in part A and 100 μm in parts B, C, and D. Parts A and C are in plane-polarized light.

pockets of MT microspar, partitioned by carbonaceous films (cf. O'Connor 1972).

At the outcrop scale, MT ribbons typically become diffuse or disappear within sandy layers. In thin section, MT ribbons similarly disappear upward within coarse-grained layers, yet are frequently represented by the presence of carbonate microspar which, rather than filling distinct cracks, fills available intergranular pore space (Fig. 6C, D). Typically, the concentration of microspar cement within the substrate becomes less dense away from adjacent MT structures. When observed under cathodoluminescence, pore-filling microspar contains dully luminescent, subrounded cores and more brightly luminescent, polygonal overgrowths, which are characteristic of crack-filling MT microspar. In several cases, where MT ribbons intersect coarse-grained siliciclastic layers, sand grains detritally fill the underlying MT voids (Fig. 7), suggesting that coarse-grained laminae were unconsolidated or only weakly bound at the time of MT crack formation. In these examples, MT microspar fills the lower portion of MT cracks and occurs throughout pore space of both the coarse-grained lamina and detrital crack fill. In rare cases, MT ribbons continue into overlying fine-grained sediment, where they, once again, are filled with MT microspar (Fig. 7).

In these latter examples, MT microspar is observed not only as a crack-filling precipitate but also as pore filling within coarse-grained facies. Pore-filling MT microspar, confirmed by CL characteristics, also occurs above horizontal ribbons passing through, or tracking, coarse-grained laminae (Fig. 6D), and within fine-grained matrix surrounding well-defined ribbons, where it typically decreases in density away from MT cracks (Fig. 8A, B). In more extreme cases, MT microspar, again confirmed by CL characteristics, occurs as the primary, pore-filling component of oolitic (Fig. 8C, D) and intraclastic grainstone lithologies that are not associated with underlying MT structures.

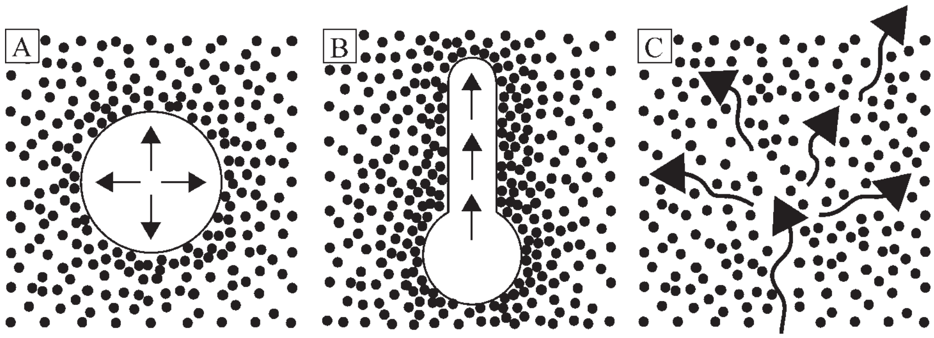

FIG. 9.—Conceptual model for the origin of MT cracks by the microscale gas–sediment interactions. **A)** If the gas pressures locally exceed the strength of grain–grain contacts, sediment is deformed to produce a gas void significantly larger than average sediment grain size. **B)** Upon further increases in gas pressure, inhomogeneities in the substrate can trigger crack formation, resulting in ribbon morphologies that propagate either upward, toward the sediment–water interface, or along low-strength anisotropies in the substrate. **C)** When gas pressures greatly exceed the strength of an unconsolidated substrate, gas movement can cause wholesale disruption (i.e., fluidization) of sediment, resulting in a disappearance of well-defined MT cracks.

INTERPRETATION

Constraints on Formation of Molar-Tooth Cracks

Petrographic examination of MT structures supports outcrop-scale and hand-sample-scale observations (Bell 1966; Smith 1968; O'Connor 1972; Fairchild et al. 1997; Winston and Lyons 1997) that suggest a strong relationship between morphology of MT cracks and the nature of the sedimentary substrate. Observations of lateral offset of vertical MT cracks at bedding planes or within coarser-grained siltstone or sandstone layers, termination of cracks beneath clay- or organic-rich horizons, grain collapse into underlying MT cracks, and the presence of MT microspar as a pore-filling precipitate suggest that grain size, substrate lithology, and substrate cohesion all play critical roles in the development of MT cracks. By contrast, the presence of a wide range of MT crack morphologies within petrographically homogeneous substrates, and an apparent relationship between crack diameter and sinuosity, suggests that the void-forming process itself also plays a role in determining the final morphology of MT cracks. Finally, the unique petrographic character of MT microspar implies *in situ* precipitation of carbonate penecontemporaneously with or soon after crack formation, and suggests a genetic relationship between the mechanism of void formation and lithification. Together, these petrographic observations are most consistent with an expanded gas expansion and migration model for MT genesis (see below; cf. Furniss et al. 1998; Marshall and Anglin 2004) wherein crack morphology is controlled by gas pressure and microscale gas–sediment interactions, and crack lithification is initiated by interactions between gas and pore fluids.

A Model for Microscale Gas–Sediment Interaction

In order to more fully understand the genesis of MT structures, it is necessary to examine the theoretical behavior of undissolved gas within an unlithified (i.e., unconsolidated) sediment matrix. The primary parameter determining gas behavior within unconsolidated sediment is the relative size of gas bubbles and sedimentary particles (Terzaghi 1944). If gas bubbles are small relative to sediment grain size, they reside within normal intergranular pore space. Although the presence of small gas bubbles alters the compressibility of the pore fluids and therefore affects the strength and mechanical behavior of the sedimentary package (Anderson and Hampton 1980; Chang and Duncan 1983; Okusa 1985; Briggs and Richardson 1996), they do not distort the internal structure of the sediment. By contrast, if gas bubbles are much larger than the sediment grain size, the internal structure of the sediment is affected by gas pressures during the consolidation and migration of gas bubbles, which impart local stress concentrations at the grain scale (Whelan et al. 1977; Wheeler 1988; Sills et al. 1991; Sills and Gonzalez 2001; Johnson et al. 2002; Boudreau et al. 2005). Sediment behavior in response to local, gas-induced stress is in turn related to the strength of the sediment, which is affected by substrate lithology (e.g., electrostatic forces between clay particles), grain size, shape, and packing (e.g., frictional forces at grain–grain contacts), organic content (e.g., grain adhesion), cementation, and any anisotropies related to changes in substrate composition (Ferm et al. 1990; Mitchener and Torfs 1996).

With these parameters, a simple conceptual model for gas–sediment interaction (Wheeler 1988; Sills et al. 1991; Briggs and Richardson 1996; Sills and Gonzalez 2001; Johnson et al. 2002; Gardiner et al. 2003; Boudreau et al. 2005) can be used to predict the formation of gas-induced cracks within a sedimentary substrate. Gas production within the substrate results in an increase in the concentration of dissolved gas within pore fluids. When saturation is reached, bubbles form that are, initially, small with respect to intergranular pores. Bubbles then grow or shrink, depending on rates of gas production, to maintain an equilibrium concentration of dissolved gas within pore fluids. Initial, small bubbles can either reside within pore space or move freely through interconnected pore space, driven by the buoyancy of the bubbles or carried by water flow through the sediment. When bubble sizes approach that of available pore space, gas pressures rise until a critical stress intensity is reached, upon which grain displacement occurs, resulting in a gas-filled void that is large with respect to sediment grain size (Fig. 9A). Stresses imparted by gas pressures within these larger bubbles compact grains along the void edge, thereby increasing local sediment strength along the bubble margin.

With sustained gas production, gas pressures continue to rise until a new critical stress threshold is reached, at which point gas pressures surpass sediment strength and migrate via displacement of surrounding sediment grains (Fig. 9B). Although buoyancy favors bubble migration towards the sediment–water interface, bubble migration is a dynamic process that depends not only on the strength of the local substrate but also on changes in gas pressure within the bubble. In a high-strength substrate, such as a substrate containing a significant proportion of clay ($>$ 15% clay greatly increases the strength of unconsolidated sediments, reaching a maximum at 20–50% clay content; Mitchener and Torfs 1996) bubbles tend to remain confined by the surrounding substrate until relatively high gas pressures are reached, at which point, failure of the substrate results in straight crack formation. In the case of organic binding of sediment lamina or interlamination of thin clay drapes, sediment packages might have highly anisotropic strength distributions that favor development of voids that track bedding defined by clay drapes or organic laminae. By contrast, in substrates of relatively low strength, gas migration follows a pathway defined by microscale differences in the strength of grain–grain contacts, potentially resulting in formation of a variety of sinuous crack patterns. Finally, upon intersecting a relatively cohesionless, low strength substrate, such as a well-sorted quartz sand

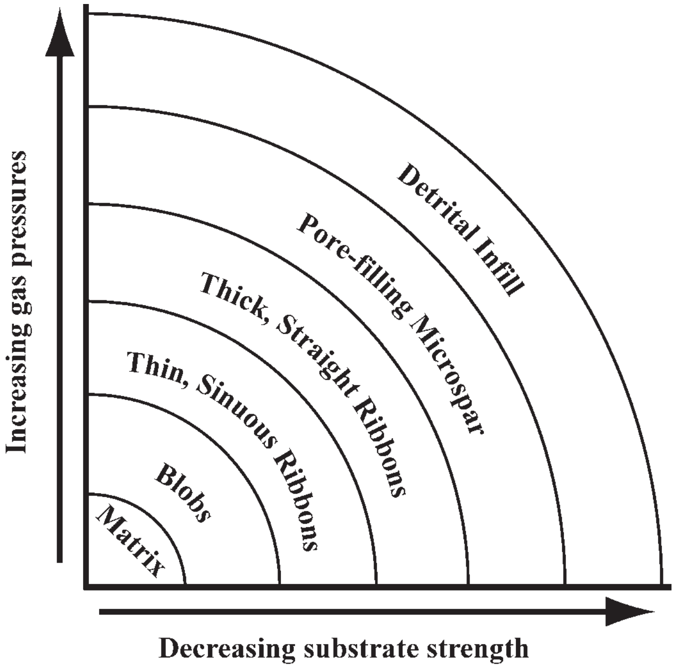

FIG. 10.—Predicted continuum of MT morphologies with variable gas pressure and/or substrate strength.

layer, gas would be expected to rapidly dissipate via either passive migration through pore space or extensive grain displacement and the wholesale fluidization of the substrate (Fig. 9C).

Interpretation of Morphologies of Molar-Tooth Cracks

Morphologies of MT cracks, defined by the distribution of characteristic MT microspar and observed across substrates of differing composition, are consistent with the predicted behavior of gas movement through unconsolidated sediment. In light of this model for microscale gas–sediment interaction, the presence of a wide range of MT morphologies within the same substrate (Fig. 5) can be interpreted as spatial variation in gas production. Low gas production relative to the strength of the surrounding substrate results in the formation of spheroidal void morphologies. With increased gas production and increased gas pressure, substrate deformation results in initial formation of ribbons. In the scenario illustrated in Figure 5, thin sinuous ribbons likely represent low rates of gas production and the minimal gas pressures necessary to deform the substrate, wherein pathways of gas migration are strongly influenced by grain-scale inhomogeneities in the substrate. By contrast, thick and straight ribbons likely result from greater rates of gas production and higher gas pressures, which easily deform substrates and are therefore less affected by grain-scale anisotropies.

Similarly, observed changes in the morphology of MT cracks across lithologic changes in the substrate can be interpreted in terms of the differing rheology of the substrates. In particular, lateral deflection of MT cracks within siltstone or sandstone layers (Fig. 6B), along bedding planes, and between organic-rich laminae are interpreted to reflect gas migration along pathways of least resistance (i.e., lesser strength) within the substrate. MT cracks that disappear within coarse-grained layers and are, instead, represented only by the presence of MT microspar distributed throughout intergranular pore space (Fig. 6C, D) are interpreted to represent gas migration through a highly permeable substrate. In an extreme example, the wholesale reorganization of grains and detrital infill of the underlying crack (Fig. 7) is interpreted as resulting from gas migration and liquefaction of an unconsolidated, cohesionless sand layer.

The presence of MT microspar interstitially within fine-grained substrates that also contain distinct MT cracks (Fig. 8A, B) is more difficult to interpret. Interstitial MT microspar may represent either initial gas production in the matrix, the movement of bubbles along gradients in the concentration of dissolved gasses, or the physical migration of small gas bubbles through sediment pore space. The density of MT microspar in matrix sediment is typically greater near MT ribbons, suggesting precipitation related to a concentration gradient in dissolved gas away from the MT crack. Finally, MT microspar is also present as a pore-filling component of certain oolitic (Fig. 8C, D) and intraclastic grainstone lithologies. In contrast to most observed oolitic and intraclastic lithologies, in which intragranular space is filled with a combination of bladed fringing cement and detrital clay and carbonate, the absence of a detrital matrix component filtering in from overlying sediment layers suggests that MT microspar may have precipitated at the sediment–water interface. In this scenario, the distribution of MT microspar would be interpreted to represent gas escape across the sediment–water interface.

Ultimately, this gas-expansion model for MT genesis provides a framework for interpreting deposition and early diagenesis of sedimentary successions, in which a continuum of MT morphologies can be defined in terms of the relative gas pressures and strength of the surrounding substrate (Fig. 10). Under conditions of very high sediment strength relative to the pressures exerted by gas production, MT structures should be absent or very sparse. This scenario may be represented by randomly distributed MT microspar grains within fine-grained substrates, reflecting initial gas production within the substrate. A relative increase in gas pressures or a decrease in substrate strength results in spheroidal voids, followed by ribbon forms. Deflection of ribbons occurs along substrate inhomogeneities except when gas pressures are relatively high or when the substrate is relatively weak. Finally, active migration of gas through pore space and detrital filling of underlying MT voids occurs only when gas pressures are relatively high or and when gas bubbles interact with a relatively noncohesive substrate.

DISCUSSION

Implications for the Origin of Molar-Tooth Microspar

The distribution and petrographic characteristics of MT microspar indicate precipitation *in situ* both within MT voids and sedimentary pore space and at the sediment–water interface, penecontemporaneously with gas production and migration. Decaying organic matter within the sedimentary substrate generates a variety of biogenic gasses, including carbon dioxide, methane, and hydrogen sulfide, depending on the microbial community and the redox and nutrient conditions of the local environment (Mechalas 1974; Floodgate and Judd 1992; Jørgensen et al. 1992). Localized geochemical change resulting from gas production, however, does not appear to have been the direct catalyst for microspar precipitation. Carbon isotope data do not show any significant compositional difference between MT cement and the surrounding sediments (Frank and Lyons 1998). This suggests that addition of ^{13}C-depleted carbon to pore fluids from potential gas sources (e.g., microbial sulfate reduction, methanogenesis, or chemical oxidation of organic matter) did not play a significant role in the formation of MT microspar.

Recent precipitation experiments, however, have produced spheroidal crystals of vaterite, a hexagonal polymorph of calcium carbonate, in the presence of dissolved organic molecules (Naka et al. 1999; Naka and Chujo 2001; Dickinson et al. 2002; Kitamura 2002). In the experiments of Naka et al. (1999) and Naka and Chujo (2001), Na_2CO_3 and $CaCl_2$ were injected into laboratory vessels with and without the addition of a variety of dissolved organic molecules. After four days, precipitates were

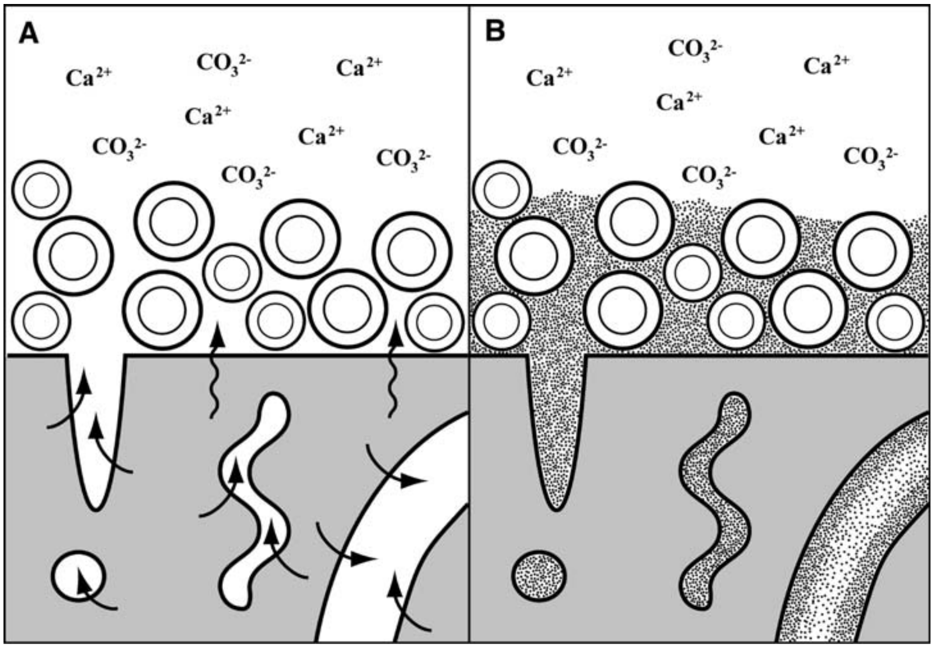

FIG. 11.—Conceptual model in which gas-induced migration of dissolved organic molecules (represented by arrows) from surrounding pore fluids may trigger precipitation of MT microspar when dissolved organics come into contact with supersaturated marine fluids. In smaller voids, MT microspar typically fills the entire void space. In larger void spaces and in the overlying seawater, precipitation of MT microspar reflects a void-ward decrease in the concentration of dissolved organic molecules.

removed and analyzed with XRD and SEM. Rather than the expected precipitation of rhombohedral calcite crystals, the addition of dissolved organics to the experiments resulted in both a larger yield of precipitated carbonate and formation of characteristic vaterite morphologies, suggesting that certain organic molecules act as a template for triggering precipitation of specific carbonate morphologies. Vaterite precipitated in these experiments was subspherical and approximately 3 µm in diameter—identical in size and morphology to the cores of MT cement observed under CL (Fig. 4B).

Gas production in the sedimentary substrate, if linked to the microbial decomposition of sedimentary organic material, should also produce a variety of dissolved organic molecules. When local water pressures exceed gas pressures, for instance directly following crack formation and expansion of the void space, fluids from the surrounding sediment and/or overlying water column rapidly floods MT voids. A contribution of fluids from the overlying water column, in particular, could provide levels of carbonate saturation necessary for rapid precipitation of vaterite crystals upon mixing with dissolved organic molecules from the surrounding sediment, producing the characteristic texture and morphology of MT microspar. In this scenario, the absence of a C-isotope signature related to microbial decomposition would be consistent with a contribution of isotopically light carbon from decomposing organic matter that was small relative to ambient concentrations of dissolved inorganic carbon (DIC) in supersaturated Mesoproterozoic and early Neoproterozoic seawater. Bartley and Kah (2004) recently suggested that both the Proterozoic marine isotopic record and patterns of Proterozoic carbonate deposition are best explained by marine elevated DIC concentrations in the latter Proterozoic (two to ten times that of the modern ocean), which acted to sustain elevated carbonate saturations. Under such elevated carbonate saturation, contributions from dissolved gases resulting from organic decomposition likely had little effect on the carbonate-producing environment. Rather, dissolved organic molecules would serve as a favorable substrate for the heterogeneous nucleation of carbonate microspar. Even relatively high concentrations of dissolved organic matter would likely catalyze, rather than participate in, microspar formation, and thus would not contribute to the isotopic composition of resultant carbonate (cf. Frank and Lyons 1998).

In this scenario, precipitation of MT microspar occurred when concentrations of dissolved organic molecules come into contact with carbonate-saturated pore water or overlying seawater (Fig. 11). In most cases, when void fluids were oversaturated with respect to carbonate, MT microspar would be expected to fill the entire void space, perhaps as a colloid, resulting in the archetypical MT structure (Furniss et al. 1998). Internal layering of MT cement in larger voids (Fig. 11; cf. vermicular structures of Moussine-Pouchkine and Bertrand-Sarfati 1997) may represent lower carbonate saturation of void fluids or a strong concentration gradient along the void edge of the dissolved organics necessary for the nucleation of MT microspar. Such a concentration gradient might result in precipitation of MT microspar as a discrete layer along the void edge, with successive precipitation events resulting in a layered structure of the void fill. At the sediment–water interface, where marine fluids are expected to be oversaturated with respect to carbonate, the density of MT microspar cementation might reflect a rapid decrease in the concentration of templating organic molecules away from the sediment–water interface.

Distribution of Molar-Tooth Structures in the Precambrian

Temporal and spatial restriction of MT structures to Mesoproterozoic and Neoproterozoic subtidal and intertidal environments (James et al. 1998) suggests that MT records a particular set of environmental conditions promoting both formation of cracks and rapid precipitation of calcium carbonate. It has been suggested that the absence of MT structure from younger Phanerozoic strata may be related to the onset of bioturbation (Frank and Lyons 1998), which would have disrupted and/or destroyed any voids generated in soft sediment. However, the last occurrence of volumetrically abundant MT ~ 750 Ma (Shields 2002) is well before the onset of significant sediment bioturbation ~ 550 Ma (Droser et al. 1999). This suggests that the distribution of MT is related to the particular environmental conditions necessary for the precipitation of its uniform microspar fill (cf. Shields 2002). Indeed, the preservation of MT structures requires rapid and early precipitation of microspar; otherwise, voids created in unlithified host substrates would simply close during later compaction (cf. Pope et al. 2003). Although gas production within sediment has certainly occurred throughout geologic history, no

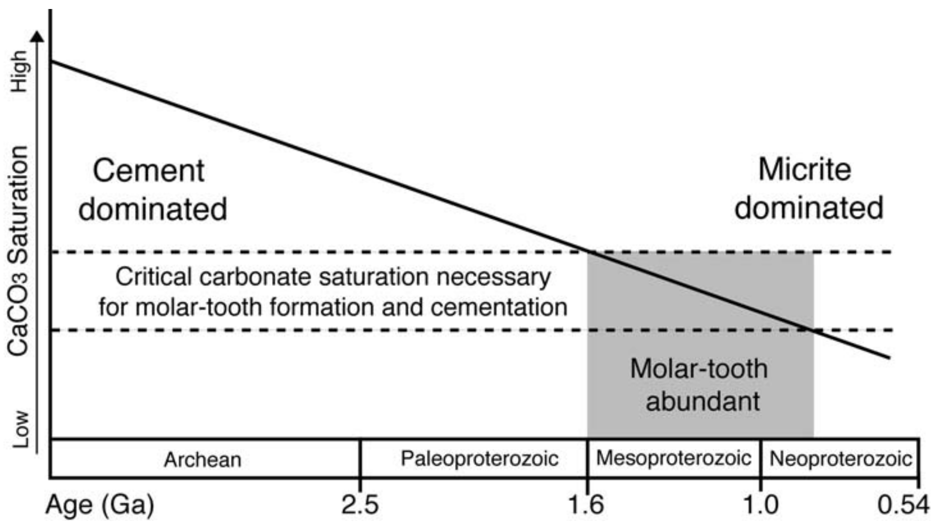

FIG. 12.—Illustration showing a hypothetical decrease in marine carbonate saturation through the Proterozoic, as represented by the relative proportion of seafloor precipitate and micritic lithologies (Kah and Knoll 1996). Abundance of MT structures in the Mesoproterozoic and early Neoproterozoic (shaded region) may reflect a critical level of marine carbonate saturation low enough to inhibit rapid substrate lithification, thereby permitting voids to form, yet high enough to facilitate precipitation of MT microspar in gas-generated voids and permeable pore space.

evidence of gas expansion would persist without the ability to preserve void space.

Inferred secular changes in marine carbonate saturation though the Precambrian may have played a critical role in the distribution of MT. Data support a transition from hard substrates in the Archean and Paleoproterozoic (i.e., those dominated by *in situ* precipitation of calcium carbonate) to soft substrates by the late Neoproterozoic (i.e., those dominated by deposition of micritic carbonate produced in the water column). This transition has been interpreted to reflect a long-term decrease in marine carbonate saturation throughout the Precambrian (Grotzinger 1989; Kah and Knoll 1996; Grotzinger and Knoll 1999), with the Mesoproterozoic to earliest Neoproterozoic representing a transitional period between these two states (Kah and Knoll 1996; Kah et al. 2001; Bartley and Kah 2004). That MT structures were most abundant during this transitional period may relate directly to changing carbonate saturation and its influence on the sedimentary substrate (Fig. 12). Mesoproterozoic to early Neoproterozoic oceans may have had a critical level of marine carbonate saturation such that minor perturbations in the physiochemical environment may have easily reduced or enhanced carbonate precipitation. Abundance of MT during this period may therefore reflect the ability of a particular environment to induce rapid precipitation of microspar into gas-generated voids. Rapidly lithified carbonate substrates of the Archean and Paleoproterozoic likely had strengths too great to permit plastic deformation during gas expansion and migration, whereas carbonate saturation may have been too low in late Neoproterozoic sediment to induce calcite precipitation within MT voids, even in the presence of high concentrations of dissolved organic matter. This hypothesis, however, does not exclude the possibility that, in certain environments, formation of MT may have been possible outside the primary MT "window" (James et al. 1998). For example, MT structures occur within spatially restricted environments of the Archean Transvaal Supergroup (Bishop and Sumner 2002). Here, an atypical occurrence of MT is present entirely within siliciclastic host rocks rather than in a mixed carbonate–siliciclastic substrate. These shaly lithologies likely were cemented less rapidly than was typical for carbonate deposits in the Archean, thereby allowing plastic deformation and MT crack formation.

This hypothesis suggests that Mesoproterozoic and early Neoproterozoic environments that promoted rapid lithification of void space, but where immediate substrate lithification was limited, should have contained a greater abundance of MT structures. Indeed, MT structures in Mesoproterozoic and early Neoproterozoic strata appear to be restricted to subtidal and lower intertidal deposits (James et al. 1998). Rapid lithification of highly evaporitic nearshore environments and slower lithification and/or lower rates of organic matter production and decomposition in offshore environments (Kah and Knoll 1996; Bartley et al. 2000) may have inhibited MT formation and/or preservation in these deposits, whereas shallow-marine environments were ideal environments for formation and preservation of MT. Smaller-scale environmental control on MT distributions are observed in the Helena Formation, where MT structures occur predominantly within upper, dolomitic portions of shoaling cycles and are rare to absent in basal, deeper-water siliciclastic strata.

CONCLUSIONS

Petrographic examination of MT structures and the distribution of MT microspar supports outcrop-scale and hand-sample-scale observations that suggest a strong relationship between the morphology of MT cracks and the nature of the sedimentary substrate. Observations are most consistent with a gas expansion and migration model for MT genesis wherein crack morphology is controlled by gas pressure and microscale gas–sediment interactions, and crack lithification results from *in situ* carbonate precipitation within voids. Interaction between migrating gas, generated by decaying organic matter within fine-grained substrates, at or near the sediment–water interface, and a variably cohesive substrate produced a predictable array of void morphologies. In the absence of continuously high rates of gas production, flooding of MT voids by fluids from the surrounding substrate and/or the overlying water column would immediately follow crack formation. An increased concentration of dissolved organic molecules, migrating into voids and the overlying water column from sedimentary pore fluids, likely induced nucleation and precipitation of subrounded vaterite crystals. Initial vaterite precipitation provided nucleation points for later calcium carbonate overgrowths, which cemented the entire void space. Prior to secondary cementation, some MT structures may have been deformed plastically, although sedimentological evidence suggests that most MT structures were lithified prior to compaction of surrounding sediment and that folded morphologies represent intrinsically sinuous pathways determined by gas–substrate interactions.

Temporal and spatial restriction of MT structures, largely to Mesoproterozoic and early Neoproterozoic shallow marine deposits, likely reflects the history of global marine carbonate saturation. High levels of carbonate saturation and very rapid lithification of substrates in the Archean and Paleoproterozoic would have resulted, except in restricted environments, in substrates whose strength greatly exceeded that which could be deformed by migrating gas. In the Mesoproterozoic to early Neoproterozoic, a critical level of carbonate saturation limited immediate substrate lithification, thereby allowing deformation of the substrate by migrating gas, yet facilitated precipitation of MT microspar within gas-generated voids and permeable pore space, given the presence of an appropriate nucleation mechanism. Decreased carbonate saturation in the late Neoproterozoic may have inhibited environmental catalysts from inducing microspar precipitation within gas-generated void space. Without rapid lithification, MT voids would have been destroyed during postdepositional compaction.

ACKNOWLEDGMENTS

This manuscript represents a portion of MDP's M.S. thesis at the University of Tennessee. Field work was aided financially by grants to MDP from the Belt Association, Tobacco Root Geological Society (Jack Harrison scholarship), Sigma Xi, Geological Society of America Southeast Section, and the University of Tennessee (Graduate Teaching Assistantship and SARIF Graduate Research Assistantship award). We thank the National Park Service for allowing sample collection in Glacier National Park, P. Schuneman for field assistance, S. Driese for helpful comments, and D. Winston for many fruitful discussions about MT structures. We also graciously thank C. Cowan, P. Myrow, D. Sumner, and J. Southard for encouragement, thoughtful criticism, and careful editing that helped to clarify and improve the manuscript.

REFERENCES

Anderson, A.L., and Hampton, L.D., 1980, Acoustics of gas-bearing sediments: Acoustical Society of America, Journal, v. 67, p. 1865–1903.

Bartley, J.K., 1996, Actualistic taphonomy of cyanobacteria: implications for the Precambrian fossil record: Palaios, v. 11, p. 571–586.

Bartley, J.K., and Kah, L.C., 2004, Marine carbon reservoir, C_{org}–C_{carb} coupling, and the Proterozoic carbon isotope record: Geology, v. 32, p. 129–132.

Bartley, J.K., Knoll, A.H., Grotzinger, J.P., and Sergeev, V.N., 2000, Lithification and fabric genesis in precipitated stromatolites and associated peritidal carbonates, Mesoproterozoic Billyakh Group, Siberia, *in* Grotzinger, J.P., and James, N.P., eds., Carbonate Sedimentation and Diagenesis in the Evolving Precambrian World: SEPM, Special Publication 67, p. 59–73.

Bauerman, H., 1885, Report on the geology of country near the forty-ninth parallel of the north latitude west of the Rocky Mountains: Geological Survey of Canada, Report of Progress 1882–84, pt. B, p. 1–42.

Bell, R.T., 1966. Precambrian rocks of the Tuchodi Lakes map-area, northeastern British Columbia, Canada [unpublished Ph.D. thesis]: Princeton University, 138 p.

Bishop, J.W., and Sumner, D.Y., 2002, Constraints on molar tooth structure from the Neoarchean Monteville Formation (abstract): Geological Society of America, Abstracts with Programs, v. 34, p. 335.

Boudreau, B.P., Algar, C., Johnson, B.D., Croudace, I., Reed, A., Furukawa, Y., Dorgan, K.M., Jumars, P.A., Grader, A.S., and Gardiner, B.S., 2005, Bubble growth and rise in soft sediments: Geology, v. 33, p. 517–520.

Briggs, K.B., and Richardson, M.D., 1996, Variability in *in situ* shear strength of gassy muds: Geo-Marine Letters, v. 16, p. 189–195.

Calver, C.R., and Baillie, P.W., 1990, Early diagenetic concretions associated with intrastratal shrinkage cracks in an upper Proterozoic dolomite, Tasmania, Australia: Journal of Sedimentary Petrology, v. 60, p. 293–305.

Chang, C.S., and Duncan, J.M., 1983, Consolidation analysis for partly saturated soil using an elastic–plastic effective stress–strain model: International Journal of Numerical Analytical Methods in Geomechanics, v. 7, p. 39–55.

Cowan, C.A., and James, N.P., 1992, Diastasis cracks: mechanically generated synaeresis-like cracks in the Upper Cambrian shallow water oolite and ribbon carbonates: Sedimentology, v. 39, p. 1101–1118.

Crawford, J.C., and Kah, L.C., 2004, Investigating the origin of Precambrian molar-tooth carbonate (abstract): Geological Society of America, Abstracts with Programs, v. 36, p. 251.

Daly, R.A., 1912, Geology of the North American Cordillera at the forty-ninth parallel: Geological Survey of Canada, Memoir 38.

Demicco, R.V., and Hardie, L.A., 1994, Sedimentary Structures and Early Diagenetic Features of Shallow Marine Carbonate Deposits: SEPM, Atlas Series, v. 1, p. 68–71.

Dickinson, S.R., Henderson, G.E., and McGrath, K.M., 2002, Controlling the kinetic versus thermodynamic crystallization of calcium carbonate: Journal of Crystal Growth, v. 244, p. 369–378.

Droser, M.L., Gehling, J.G., and Jenson, S., 1999, When the worm turned: concordance of Early Cambrian ichnofabric and trace-fossil record in siliciclastic rocks of South Australia: Geology, v. 27, p. 625–628.

Dunham, R.J., 1969, Early vadose silt in Townsend mound (reef), New Mexico, *in* Friedman, G.M., ed., Depositional Environments in Carbonate Rocks: SEPM, Special Publication 14, p. 139–181.

Eby, D.E., 1977. Sedimentation and early diagenesis within eastern portions of the "Middle Belt Carbonate Interval" (Helena Formation), Belt Supergroup (Precambrian Y), western Montana [unpublished Ph.D. thesis]: State University of New York: Stony Brook, 712 p.

Evans, K.V., Aleinikoff, J.N., Obradovich, J.D., and Fanning, C.M., 2000, SHRIMP U–Pb geochronology of volcanic rocks, Belt Supergroup, western Montana: evidence for rapid deposition of sedimentary strata: Canadian Journal of Earth Sciences, v. 37, p. 1287–1300.

Fairchild, I.J., Einsele, G., and Song, T., 1997, Possible seismic origin of molar tooth structures in Neoproterozoic carbonate ramp deposits, north China: Sedimentology, v. 44, p. 611–636.

Ferm, J.B., Erlich, R., Kranz, R.L., and Park, W.C., 1990, The relationship between petrographic image analysis data and fracture toughness: Association of Engineering Geologists, Bulletin, v. 27, p. 327–339.

Floodgate, G.D., and Judd, A.G., 1992, The origins of shallow gas: Continental Shelf Research, v. 12, p. 1145–1156.

Frank, T.D., and Lyons, T.W., 1998, "Molar-tooth" structures: A geochemical perspective on a Proterozoic enigma: Geology, v. 26, p. 683–686.

Furniss, G., Rittel, J.F., and Winston, D., 1998, Gas bubble and expansion crack origin of "molar-tooth" calcite structures in the Middle Proterozoic Belt Supergroup, western Montana: Journal of Sedimentary Research, v. 68, p. 104–114.

Gardiner, B.S., Boudreau, B.P., and Johnson, B.D., 2003, Growth of disk-shaped bubbles in sediments: Geochimica et Cosmochimica Acta, v. 67, p. 1485–1494.

Grotzinger, J.P., 1986, Shallowing-upward cycles of the Wallace Formation, Belt Supergroup, northwestern Montana and northern Idaho, *in* Roberts, S.M., ed., A Guide to Proterozoic Rocks of Western Montana and Adjacent Areas: Montana Bureau of Mines and Geology, Special Publication 94, p. 143–160.

Grotzinger, J.P., 1989, Facies and evolution of Precambrian carbonate depositional systems: emergence of the modern platform archetype, *in* Crevello, P.D., Wilson, J.J., Sarg, J.F., and Read, J.F., eds., Controls on Carbonate Platform and Basin Development: SEPM, Special Publication 44, p. 79–106.

Grotzinger, J.P., and Knoll, A.H., 1999, Stromatolites in Precambrian carbonates: evolutionary mileposts or environmental dipsticks?: Annual Review of Earth and Planetary Sciences, v. 27, p. 313–358.

Hofmann, H.J., 1985, The mid-Proterozoic Little Dal macrobiota, Mackenzie Mountains, Northwest Canada: Palaeontology, v. 28, p. 331–354.

Horodyski, R.J., 1976, Stromatolites of the upper Siyeh Limestone (Middle Proterozoic), Belt Supergroup, Glacier National Park, Montana: Precambrian Research, v. 3, p. 517–536.

Horodyski, R.J., 1983, Sedimentary geology and stromatolites of the Middle Proterozoic Belt Supergroup, Glacier National Park, Montana: Precambrian Research, v. 20, p. 391–425.

James, N.P., Narbonne, G.M., and Sherman, A.B., 1998, Molar-tooth carbonates: shallow subtidal facies of the Mid- to Late Proterozoic: Journal of Sedimentary Research, v. 68, p. 716–722.

Johnson, B.D., Boudreau, B.P., Gardiner, B.S., and Maass, R., 2002, Mechanical response of sediments to bubble growth: Marine Geology, v. 187, p. 347–363.

Jørgensen, B.B., Nelson, D.C., and Ward, D.M., 1992, Chemotrophy and decomposition in microbial mats, *in* Schopf, J.W., and Klein, C., eds., The Proterozoic Biosphere; A Multidisciplinary Study: New York, Cambridge University Press, p. 287–293.

Kah, L.C., and Knoll, A.H., 1996, Microbenthic distribution of Proterozoic tidal flats: environmental and taphonomic considerations: Geology, v. 24, p. 79–82.

Kah, L.C., Lyons, T.W., and Chesley, J.T., 2001, Geochemistry of a 1.2 Ga carbonate–evaporite succession, northern Baffin and Bylot Islands: implications for Mesoproterozoic marine evolution: Precambrian Research, v. 111, p. 203–234.

Kile, D.E., Eberl, D.D., Hoch, A.R., and Reddy, M.M., 2000, An assessment of calcite crystal growth mechanisms based on crystal size distributions: Geochimica et Cosmochimica Acta, v. 64, p. 2937–2950.

Kitamura, M., 2002, Controlling factor of polymorphism in crystallization process: Journal of Crystal Growth, v. 237–239, p. 2205–2214.

Marshall, D., and Anglin, C.D., 2004, CO_2-clathrate destabilization: a new model of formation for molar tooth structures: Precambrian Research, v. 129, p. 325–341.

Mechalas, B.J., 1974, Pathways and environmental requirements for biogenic gas production, *in* Kaplan, I.R., ed., Natural Gasses in Marine Sediments: New York, Plenum Press, p. 11–25.

Mitchener, H., and Torfs, H., 1996, Erosion of mud/sand mixtures: Coastal Engineering, v. 29, p. 1–25.

Moussine-Pouchkine, A., and Bertrand-Sarfati, J., 1997, Tectonosedimentary subdivisions in the Neoproterozoic to Early Cambrian cover of the Taoudenni basin (Algeria–Mauritania–Mali): Journal of African Earth Sciences, v. 24, p. 426–443.

Naka, K., and Chujo, Y., 2001, Control of crystal nucleation and growth of calcium carbonate by synthetic substrates: Chemical Materials, v. 13, p. 3245–3259.

Naka, K., Tanaka, Y., Chujo, Y., and Ito, Y., 1999, The effect of an anionic starburst dendrimer on the crystallization of $CaCO_3$ in aqueous solution: Chemical Communications, p. 1931–1932.

O'Connor, M.P., 1972, Classification and environmental interpretation of the cryptalgal organosedimentary "molar-tooth" structure from the Late Precambrian Belt–Purcell Supergroup: Journal of Geology, v. 80, p. 592–610.
Okusa, S., 1985, Wave-induced stresses in unsaturated marine sediments: Géotechnique, v. 35, p. 517–532.
Pope, M.C., Bartley, J.K., Knoll, A.H., and Petrov, P.Y., 2003, Molar-tooth structures in calcareous nodules, early Neoproterozoic Burovaya Formation, Turukhansk Region, Siberia: Sedimentary Geology, v. 158, p. 235–248.
Pratt, B.R., 1998, Molar-tooth structure in Proterozoic carbonate rocks: Origin from synsedimentary earthquakes, and implications for the nature and evolution of basins and marine sediment: Geological Society of America, Bulletin, v. 110, p. 1028–1045.
Pratt, B.R., 2001, Oceanography, bathymetry and syndepositional tectonics of a Precambrian intracratonic basin: integrating sediments, storms, earthquakes and tsunamis in the Belt Supergroup (Helena Formation, ca. 1.45 Ga), western North America: Sedimentary Geology, v. 141–142, p. 371–394.
Shields, G.A., 2002, "Molar-tooth microspar": a chemical explanation for its disappearance ~ 750 Ma: Terra Nova, v. 14, p. 108–113.
Sills, G.C., and Gonzalez, R., 2001, Consolidation of naturally gassy soft soil: Géotechnique, v. 51, p. 629–639.
Sills, G.C., Wheeler, S.J., Thomas, S.D., and Gardner, T.N., 1991, Behaviour of offshore soils containing gas bubbles: Géotechnique, v. 41, p. 227–241.
Smith, G.A., 1968, The origin and deformation of some "molar-tooth" structures in the Precambrian Belt–Purcell Supergroup: Journal of Geology, v. 76, p. 426–443.
Smith, S.V., and Winston, D., 1997, Formation of cracks in subaqueous fluid mud by solitary waves, central Louisiana Gulf of Mexico coast (abstract): Geological Society of America, Abstracts with Programs, v. 29, p. 440.
Terzaghi, K., 1944. Theoretical Soil Mechanics: London, Wiley, 510 p.
Wheeler, S.J., 1988, A conceptual model for soils containing large gas bubbles: Géotechnique, v. 38, p. 389–397.
Whelan, T., Coleman, J.M., Suhayda, J.N., and Roberts, H.H., 1977, Acoustical penetration and shear strength in gas-charged sediment: Marine Geotechnology, v. 2, p. 147–159.
Winston, D., 1986, Sedimentology of the Ravalli Group, Middle belt Carbonate and Missoula Group, Middle Proterozoic Belt Supergroup, Montana, Idaho, and Washington, *in* Roberts, S.M., ed., A Guide to Proterozoic Rocks of Western Montana and Adjacent Areas: Montana Bureau of Mines and Geology, Special Publication 94, p. 143–160.
Winston, D., and Link, P.K., 1993, Middle Proterozoic rocks of Montana, Idaho, and eastern Washington: The Belt Supergroup, *in* Reed, J.C., Bickford, M.E., Houston, R.S., Link, P.K., Rankin, D.W., Sims, P.K., and Van Schums, W.R., eds., Precambrian: Conterminous U.S.: The Geology of North America, v. C-2: Geological Society of America, Decade of North American Geology, p. 487–517.
Winston, D., and Lyons, T., 1997, Sedimentary cycles in the St. Regis, Empire and Helena formations of the Middle Proterozoic Belt Supergroup, northwestern Montana, *in* Link, P.K., ed., Geologic Guidebook to the Belt–Purcell Supergroup, Glacier National Park and Vicinity, Montana and Adjacent Canada, Field Trip Guidebook for the Belt Symposium III Whitefish: Montana, p. 21–51.
Winston, D., Woods, M., and Byer, G.B., 1984, The case for an intracratonic Belt–Purcell basin: tectonic, stratigraphic and stable isotopic considerations, *in* McBane, J.D., and Garrison, P.B., eds., Northwest Montana and Adjacent Canada: Montana Geological Society, Field Conference Symposium, p. 103–118.
Young, G.M., and Long, D.G.F., 1977, Carbonate sedimentation in a late Precambrian shelf sea, Victoria Island, Canadian Arctic Archipelago: Journal of Sedimentary Petrology, v. 47, p. 943–955.

Received 4 March 2005; accepted 1 July 2005.